NeuroImage: Clinical 19 (2018) 727–733

Contents lists available at ScienceDirect

NeuroImage: Clinical

journal homepage: www.elsevier.com/locate/ynicl

Cortical thickness analysis in operculo-insular epilepsy

Sami Obaid[a,b,c], Alan Tucholka[d], Jimmy Ghaziri[b,e], Pierre-Marc Jodoin[f], Félix Morency[f], Maxime Descoteaux[f], Alain Bouthillier[c], Dang K. Nguyen[a,b,g,*]

[a] Département de Neurosciences, Université de Montréal, Montréal, Québec, Canada
[b] Centre de Recherche du Centre Hospitalier de l'Université de Montréal, Montréal, Québec, Canada
[c] Service de Neurochirurgie, Centre Hospitalier de l'Université de Montréal, Montréal, Québec, Canada.
[d] Barcelona Beta Brain Research Center, Foundation Pasqual Maragall, Barcelona, Spain
[e] Département de psychologie, Université du Québec à Montréal, Montréal, Québec, Canada
[f] Sherbrooke Connectivity Imaging Lab (SCIL), Université de Sherbrooke, Sherbrooke, Québec, Canada
[g] Service de Neurologie, Centre Hospitalier de l'Université de Montréal, Montréal, Québec, Canada

ARTICLE INFO

Keywords:
Epilepsy
Insula
Operculum
Cortical thickness

ABSTRACT

Background: In temporal lobe epilepsy (TLE), advanced neuroimaging techniques reveal anomalies extending beyond the temporal lobe such as thinning of fronto-central cortices. Operculo-insular epilepsy (OIE) is an under-recognized and poorly characterized condition with the potential of mimicking TLE. In this work, we investigated insular and extra-insular cortical thickness (CT) changes in OIE.

Methods: All participants (14 patients with refractory OIE, 9 age- and sex-matched patients with refractory TLE and 26 healthy controls) underwent a T1-weighted acquisition on a 3 T MRI. Anatomical images were processed with Advanced Normalization Tools. Between-group analysis of CT was performed using a two-sided *t*-test (threshold of $p < 0.05$ after correction for multiple comparisons; cut-off threshold of 250 voxels) between (i) patients with OIE vs TLE, and (ii) patients with OIE vs healthy controls.

Results: Significant widespread thinning was observed in OIE patients as compared with healthy controls mainly in the ipsilateral insula, peri-rolandic region, orbito-frontal area, mesiotemporal structures and lateral temporal neocortex. Contralateral cortical shrinkage followed a similar albeit milder and less diffuse pattern.

The CT of OIE patients was equal or reduced relative to the TLE group for every cortical region analyzed. Thinning was observed diffusely in OIE patients, predominantly inboth insulae and the ipsilateral occipito-temporal area.

Conclusion: Our results reveal structural anomalies extending beyond the operculo-insular area in OIE.

1. Introduction

The insular cortex is a complex integrative structure involved in a variety of functions including autonomic, sensorimotor, viscero-sensitive, cognitive and emotional functions (Nieuwenhuys, 2012; Uddin et al., 2017). Recent studies using resting-state or active tasks functional magnetic resonance imaging (fMRI) have unravelled the wide array of somatotopically organized functional circuitry of the human insula, which includes connections with temporo-limbic regions, prefrontal, orbitofrontal andpremotor cortices, supplementary motor area, primary and secondary somatosensory cortices, cingulate cortex, precuneus and occipital lobe(Cauda et al., 2011, 2014; Deen et al., 2011). Such findings were further corroborated in cortico-cortical evoked potential studies (Almashaikhi et al., 2014) and diffusion tractography studies revealing extensive multilobar connections with the insula (Cerliani et al., 2012; Cloutman et al., 2012; Ghaziri et al., 2017; Jakab et al., 2012).

The wide spectrum of insular connectivity-related functions accounts for the diverse ictal manifestations observed in operculo-insular epilepsy (OIE). Insular seizures may present with various seizure manifestations including visceral, affective, autonomic and sensory auras, motor and non-motor seizure types that can mimic parietal, frontal or temporal lobe seizures and render the clinical recognition of OIE arduous (Nguyen et al., 2009; Obaid et al., 2017). Moreover, non-invasive electrophysiological and imaging investigations including scalp electroencephalography (sEEG), ictal single-photon emission computed tomography (SPECT), positron emission tomography (PET) often fail to reveal the precise epileptic origin, eventually requiring invasive EEG monitoring to confirm the location of the epileptic focus (Gras-Combe et al., 2016; Isnard et al., 2000; Mohamed et al., 2013;

* Corresponding author at: CHUM, 1000Saint-Denis, Montreal, Quebec H2X 0C1, Canada.
E-mail address: d.nguyen@umontreal.ca (D.K. Nguyen).

https://doi.org/10.1016/j.nicl.2018.05.033
Received 3 January 2018; Received in revised form 23 May 2018; Accepted 25 May 2018
Available online 31 May 2018

Ostrowsky et al., 2000; Ryvlin et al., 2006; Weil et al., 2016). For those reasons, OIE remains a diagnostic challenge and probably under-recognized condition. In patients with drug-resistant OIE epilepsy, accurate identification may lead to successful epilepsy surgery while failure to recognize it may lead to resection of the wrong area and poor post-operative seizure outcome(Nguyen et al., 2009; Obaid et al., 2017; Surbeck et al., 2010; Alomar et al., 2017; Bouthillier and Nguyen, 2017; Freri et al., 2017; Malak et al., 2009).

Structural MRI analysis enables in vivo evaluation of the human cortex (Bernhardt et al., 2008; Mechelli et al., 2005). Voxel-based morphometry (VBM) is a frequently used quantitative method which allows measurement of gray matter volume or density (Bonilha et al., 2010b; Li et al., 2012). However, VBM has the drawback of neglecting the curvature of the sulco-gyral distribution even when nonlinear registration is performed (Ashburner and Friston, 2000; Lin et al., 2007), ultimately leading to a reduced sensitivity for detecting differences in cortical anatomy. Submillimetric estimation of cortical thickness (CT) is a more anatomically adapted and sensitive technique that allows measurements across the non-linear pattern of the cortical surface by computing the cortical mantle according to its three-dimensional folding (Lin et al., 2007; Thompson et al., 2004; Tustison et al., 2014).

Previous studies evaluating the CT in patients with temporal lobe epilepsy (TLE) have revealed distant extra-temporal cortical atrophy of temporo-limbic and fronto-central areas, attributed to seizure propagation through the limited connections of mesiotemporal structures (Bernhardt et al., 2008, 2009, 2010; Lin et al., 2007; McDonald et al., 2008). To our knowledge however, no studies have looked at the estimation of CT in patients with OIE. Herein, we sought to assess insular and diffuse extra-insular variations of CT in patients with OIE.

2. Materials and methods

2.1. Participants

We studied 14 patients with long-standing refractory OIE (9 females; 33 ± 7 years; 19–46 years; eight right OIEs and six left OIEs) investigated at the University of Montreal Health Center. Of those 14 patients, nine had an epileptic focus involving only a subregion of the insula (six patients with an anterior insular focus and three with a posterior insular focus) and five patients had a more extensive focus involving both the anterior and posterior insulae. The epileptic focus involved one of the adjacent (frontal, temporal or parietal) operculum in all patients.

These patients were compared to two age- and sex-matched control groups composed of 26 healthy individuals with no neurological or psychiatric disorders (13 females; 28 ± 5 years; 23–40 years) and nine patients with medically intractable TLE (5 females; 27 ± 6 years; 18–36 years; four left TLEs and five right TLEs). As per standardised protocol, every epileptic participant underwent a comprehensive evaluation including a detailed history, neurological examination, review of medical records, prolonged scalp EEG-video recordings and a neuropsychological evaluation. Non-invasive imaging investigations were performed in all epileptic patients and included seizure protocol T1, T2 and Fluid-attenuated inversion recovery (FLAIR) brain MRI sequences and an ictal SPECT. In addition, magnetoencephalography (MEG) was performed in 12 OIE and three TLE patients to further characterize seizure origin. Confirmation of seizure focus required intracranial EEG recordings in 13 OIE subjects and one TLE participant. Patients with tumoral lesions or vascular anomalies were excluded in both the OIE and TLE groups. All healthy controls (HC) were scanned using the same MRI sequences as the epileptic patients.

2.2. MRI and statistical analysis

All participants underwent a T1-weighted acquisition on a 3T Achieva X MRI (Philips, the Netherlands) with the following parameters: TR = 8.1 ms; TE = 3.8 ms; flip angle = 8°; slices = 176; voxel size = 1 × 1 × 1 mm, FOV = 230 × 230 mm with an 8-channels head coil.

As performed in previous studies with TLE (Coan et al., 2014; Yasuda et al., 2010), all images of patients with right-sided OIE or TLE were side-flipped prior to pre-processing which allowed the analysis to be performed uniformly and therefore increase the sample size and the sensitivity of detecting alterations in CT.

Anatomical images were processed with Advanced Normalization Tools - ANTs (Avants et al., 2011; Tustison et al., 2014), which briefly consists in a bias correction of the T1 image, brain extraction, prior-based 6-tissue probabilistic segmentation, cortical thickness estimation and normalization on the custom template from Open Access Series of Imaging Studies (OASIS-30_Atropos - http://www.mindboggle.info/data.html). Resulting from this tool, a cortical thickness volumetric image, in the normalized space, was produced for each subject.

We then used the Statistical Parametric Mapping (SPM) software version 12 (from the Wellcome Trust Centre for Neuroimaging;http://www.fil.ion.ucl.ac.uk/spm/) to smooth cortical thickness maps (full-width at half maximum of 4 mm) and to perform the second-level analysis in the VBM method (Ashburner and Friston, 2000). We calculated statistical t-maps of the following contrasts: OIE vs. TLE and OIE vs. healthy controls (HC). In the design matrix, we added age and gender as covariates for the OIE vs. HC comparison whereas age, gender, the age at onset of epilepsy, and the duration of epilepsy were included as covariates in the OIE vs TLE analysis. Resulting maps (t-values) were exported to the xjview software (http://www.alivelearn.net/xjview) to perform the correction for multiple comparisons (false discovery rate; FDR) and automatically extract significant regions. We thresholded statistical maps at $p < 0.05$ (FDR corrected). A cut-off threshold of 250 voxels was applied in order to include large enough regions with anatomical significance.

We segmented the template obtained from ANTs with Freesurfer 5.3 (http://surfer.nmr.mgh.harvard.edu/) to create a 3D representation of the brain for visualisation purpose (Dale et al., 1999). We created a mid-surface, a new surface between the pial and white surface for a better volume-to-surface projection. All results obtained with SPM were projected to the mid-surface.

Student's *t*-test and Pearson's chi-squared test were used to compare continuous and categorical clinical variables respectively among the three groups. We used SPSS (IBM SPSS Statistics, Version 21.0, Armonk, NY) for statistical analysis of clinical variables.

3. Results

3.1. Patient population

Except for three patients with cortical dysplasia, all OIE patients had non-lesional epilepsies (11 patients) and therefore diagnosis and inclusion of OIE relied mainly on intracranial EEG monitoring findings. None of these patients exhibited sclerosis of the mesiotemporal region. All OIE participants underwent a partial or radical insular resection with or without an operculectomy (Bouthillier and Nguyen, 2017; Malak et al., 2009) with a favourable seizure outcome (Engel class I for 11 patients and II for 3; mean follow-up time 3.9 ± 2.8 years). In all cases, the resection was limited to the epileptic focus: six and three patients underwent an anterior and posterior operculo-insulectomy respectively, whereas five patients had a radical insulectomy with an operculectomy. In the active control group, all TLE patients had hippocampal sclerosis (HS) and medial temporal lobe epilepsy based on diagnostic investigations. The OIE group was statistically similar to both control groups with respect to age and gender (Table 1). In addition, OIE and TLE participants did not reveal differences regarding the age at seizure onset or duration of epilepsy (Table 1). Informed written consent was obtained from all participants and the study was approved by the University of Montreal Health Center ethics board.

Table 1
Demographic and clinical information.

	Age at MRI	Women	Onset	Duration
OIE (n = 14)	33 ± 7 (19–46)	9	17 ± 12	16 ± 12
TLE (n = 9)	27 ± 6 (18–36)	5	19 ± 9	8 ± 7
Healthy controls (n = 26)	28 ± 5 (23–40)	13	NA	NA

Age at MRI, age of onset and duration of epilepsy are presented in years ± SD (age range). No between-group statistically significant differences were observed in any variable.

3.2. Group comparison between OIE and healthy controls

Areas of significant cortical thinning in OIE as compared to HCs are shown in Fig. 1. At corrected thresholds, the CT of OIE subjects was equal or reduced relative to HCs. Relative to HCs, patients with OIE showed evidence of widespread cortical thinning. With regards to the temporal area, bilateral reduction in CT was observed in the parahippocampal and fusiform gyri, the temporal pole and the lateral temporal neocortex mainly involving but not limited to the superior temporal gyrus. Within the frontal lobe, bilateral atrophy was noted in the orbitofrontal area (orbitofrontal gyrus, rectus gyrus and olfactory cortex), the mesio-frontal area (superior frontal gyrus, supplementary motor areas and all three parts of the cingulate gyrus) and the lateral frontal cortices (including all three frontal gyri but mainly the inferior frontal gyrus). The perirolandic (precentral, postcentral and paracentral cortices), temporo-occipital (fusiform, lingual and all three occipital gyri as well as the cuneus and the pericalcarine cortex) and medial parietal regions (precuneus) were also bilaterally atrophied. Within the cerebellum, atrophy was observed on both sides, mainly in the vermis. Additional cortical thinning was detected in the ipsilateral insula and the central operculum while small and scattered clusters were observed in the contralateral supramarginal gyrus. Interestingly, the most prominent cortical atrophyseemed to be located in the perirolandic region, the orbitofrontal area and the mesiotemporal structures for both hemispheres, the superior temporal gyrus mainly ipsilateral to seizure focus and to a lesser extent the ipsilateral inferior frontal gyrus. No region of cortical hypertrophy was observed (Figs. 1 and 2).

3.3. Group comparison between OIE and TLE

Areas of significant cortical thinning in OIE as compared to TLE are shown in Fig. 2. Compared to TLE controls, analysis at corrected thresholds revealed diffuse decrease in CT for OIE patients bilaterally. Within the temporo-insular area, bilateral thinning was observed in the insula, mesiotemporal structures as well as the temporal pole and the inferior, middle and superior temporal gyri. Regarding the frontal lobe, bilateral reduction in CT was noted in mesiofrontal (anterior cingulate gyrus, middle cingulate gyrus, supplementary motor area and the superior frontal gyrus) and lateral frontal structures (superior, middle and inferior frontal gyri) as well as in the orbitofrontal area. In addition, the occipito-temporal region (occipital gyri, pericalcarine cortex, lingual gyrus, cuneus and fusiform gyrus), the ventral and dorsal perirolandic region and the cerebellum were also thinner bilaterally. Within the parietal lobe, the precuneus and both superior and inferior parietal lobules were significantly thinner in OIE than in TLE subjects on both sides. Cortical atrophy was also observed in Heschl's gyrus contralateral to seizure focus. There was no region revealing a thinner cortex in patients with TLE.

4. Discussion

We investigated the CT in a group of patients with long-standing OIE. Comparing OIE patients with HCs revealed widespread bilateral cortical thinning mainly in the insula, peri-rolandic region, orbitofrontal area, lateral temporal neocortex and mesiotemporal structures. In addition, comparing OIE and TLE patients revealed more significant atrophy in OIE predominantly in bilateral insulae and the occipitotemporal cortex.

Patients with OIE revealed widespread atrophy involving insular, temporal and extratemporal areas. Previous functional MRI investigations linked the insula to various cortical areas including mainly temporo-limbic regions and perirolandic areas, and to a lesser extent the prefrontal, parietal and visual cortices (Cauda et al., 2011; Deen et al., 2011). Further evidence of insular connectivity came from intracerebral cortical stimulation using cortico-cortical evoked potentials, which revealed insular connections with adjacent perisylvian and distant neocortical regions involving all four lobes (Almashaikhi et al., 2014). In these studies, the observed functional connectivity was likely related to

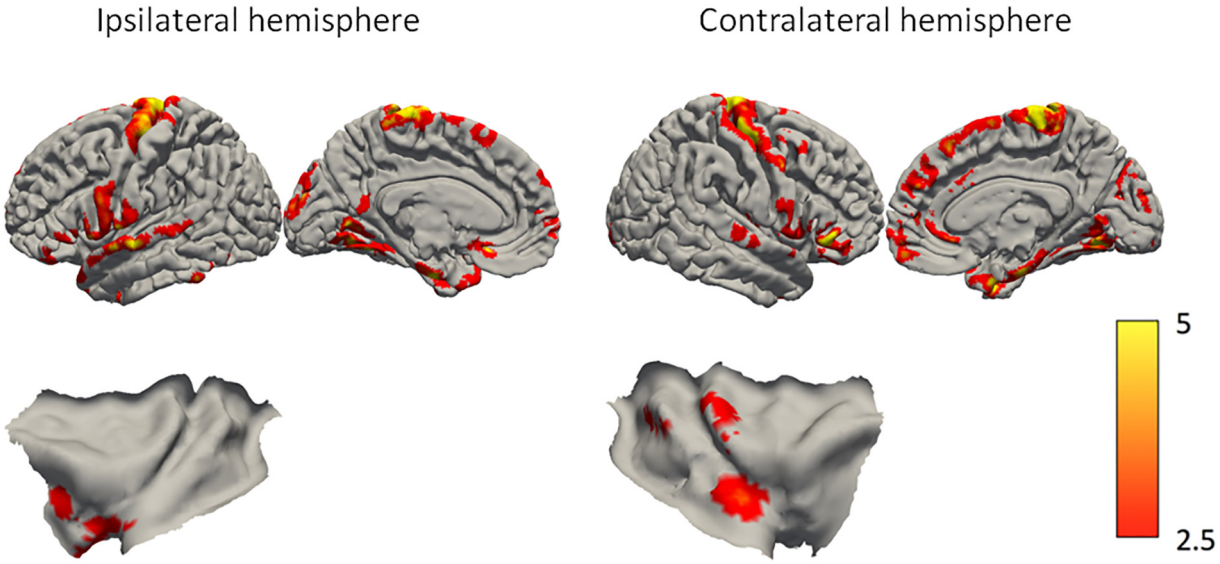

Fig. 1. Group comparison of cortical thickness between OIE participants and healthy controls. Yellow-orange regions indicate reduction of cortical thickness in OIE patients relative to healthy participants. The colour bar corresponds to the *t* values: higher *t* values represent more significant atrophy. Analysis was performed with correction for multiple comparisons using False discovery rate. Significance was thresholded at $p < 0.05$. Only clusters with a minimum of 250 voxels were included. (For interpretation of the references to color in this figure legend, the reader is referred to the web version of this article.)

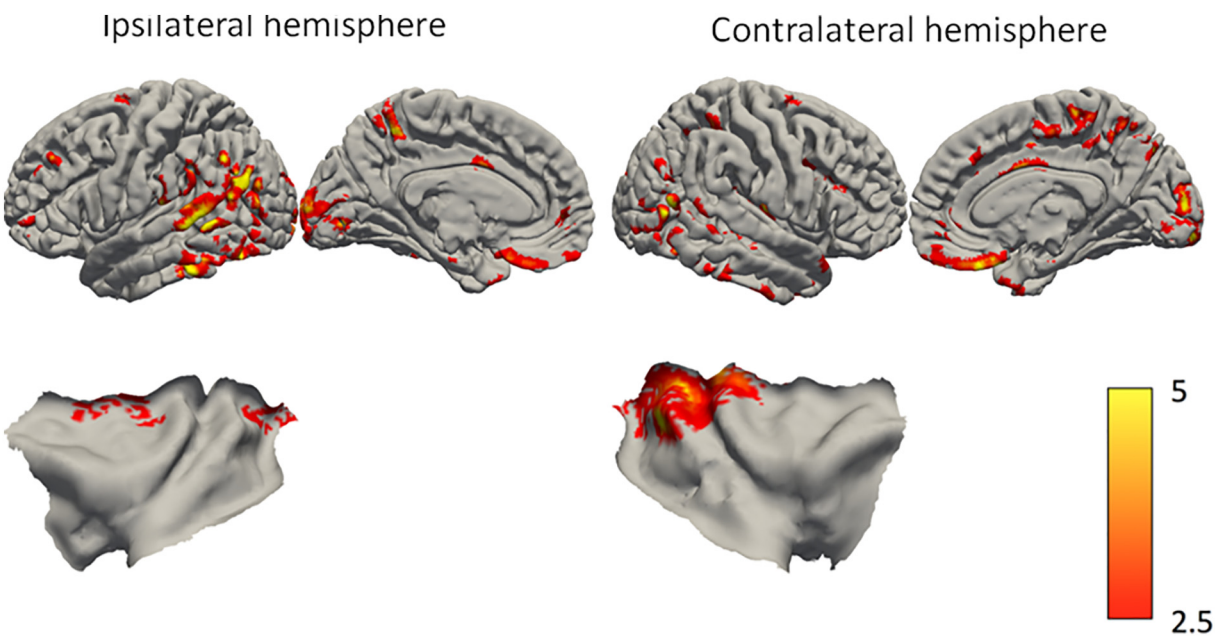

Fig. 2. Group comparison of cortical thickness between OIE and TLE participants. Yellow-orange regions indicate reduction of cortical thickness in OIE patients relative to TLE participants. The colour bar corresponds to the *t* values: higher *t* values represent more significant atrophy. Analysis was performed with correction for multiple comparisons using FDR. Significance was thresholded at $p < 0.05$. Only clusters with a minimum of 250 voxels were included. (For interpretation of the references to color in this figure legend, the reader is referred to the web version of this article.)

the white matter circuitry adjoining the insula to the extra-insular cortex (Almashaikhi et al., 2014; Cauda et al., 2011; Deen et al., 2011). Indeed, tract-tracing of the insula in nonhuman primates and human tractography studies revealed concordant widespread cortical connections originating from the insula (Ghaziri et al., 2017; Mesulam and Mufson, 1982; Mufson and Mesulam, 1982). In a recent report using tractography, Ghaziri et al. (2017) identified fibers connectingthe insula to the medial and lateral frontal, parietal, temporal and occipital lobes. If one assumes that the propagation of epileptic discharges is directly responsible for cortical thinning, it should come as no surprise that OIE leads to the observed diffuse multilobar cortical atrophy. Whelan et al. (2018) recently reported the largest neuroimaging analysis of cortical thickness for epilepsy which included patients from 24 centers with either idiopathic generalized epilepsy, focal mesiotemporal epilepsy, focal extratemporal epilepsy or other unclassified syndromes. Although patients with OIE were not included in their study, combining the results of CT in patients with temporal and extratemporal epilepsy (frontal, parietal, occipital, other focal epilepsies not otherwise specified and other unclassified syndromes) revealed widespread atrophy involving the prefrontal area, the perirolandic cortex and the medial and lateral occipital, parietal and temporal cortices. Interestingly, we observed a similar pattern of cortical thinning in patients with OIE, albeit slightly more diffuse, revealing additional atrophy in the insula, orbitofrontal and cingulate gyri. The distribution of atrophy seems to mimic the combined pattern of focal extrainsular epilepsies, further supporting the widespread multilobar connectivity of the operculo-insular area.

We also observed thinner cortical regions in patients with OIE as compared to TLE. Interestingly, we could not identify any region more atrophied in TLE patients compared to OIE patients. The observed findings may potentially be explained by a similar distribution of atrophy for both epilepsies, albeit the degree of atrophy being more severe in OIE. However, although CT analysis comparing TLE patients to HCs was not performed in our study, multiple reports have previously shown a more limited pattern of cortical thinning in TLE, predominantly involving fronto-central and temporo-limbic regions (Bernhardt et al., 2008, 2009, 2010; Lin et al., 2007; McDonald et al., 2008; Whelan et al., 2018). Alternatively, it may be possible that the differential pattern of connectivity of both regions (mesiotemporal area and operculo-insular region) is responsible for the pattern of cortical thinning. Whereas mesiotemporal structures are 'limitedly' connected, the insula exhibits a vast array of connections involving the same regions but also the lateral frontal and the medial and lateral parietal and occipital cortices (Bernhardt et al., 2008, 2009, 2010; Lin et al., 2007; McDonald et al., 2008). Such wide connectivity likely reflects the wider functional spectrum of the insula, a highly integrative region.

Whereas mesiotemporal structures are limitedly connected, the insula exhibits a vast array of connections involving the same regions but also the lateral frontal and the medial and lateral parietal and occipital cortices (Bernhardt et al., 2008, 2009, 2010; Lin et al., 2007; McDonald et al., 2008). Such wide connectivity likely reflects the wider functional spectrum of the insula, a highly integrative region.

We evaluated the CT using the latest-state-of-the-art method of cortical surface analysis, namely ANTs. Coregistration and normalization methods play a critical part in VBM studies, and poorly registered images may lead to irrational findings (Bookstein, 2001). We chose to use the ANTs software because of the symmetric diffeomorphic image registration (Avants et al., 2008) that has been indicated to be one of the best inter-individual co-registration among 14 other methods (Klein et al., 2009). Moreover, this tool produces cortical thickness maps, measured in millimeters, while tools like SPM typically create gray matter volume maps. We believe CT offers a higher inter-individual cortex-to-cortex accuracy. The diffeomorphic registration based cortical thickness (DiReCT) measure derived from ANTs is robust and well established in the literature (Tustison et al., 2014). It keeps a strong correspondence between maps even in the presence of different noise levels, has a good ability to recover buried sulci and deep curvatures, uses a volumetric diffeomorphic correspondence model, incorporates a natural geometric definition of thickness, and encodes thickness measures within the volumic domain, enabling voxel-wise statistics (Das et al., 2009).

The pathophysiology of extra-insular gray matter atrophy observed with CT analysis in epileptic patients remains uncertain. Previous electrophysiological studies in patients with TLE demonstrated that the pattern of atrophy reflects the route of seizure spreading within the temporo-limbic network (Wennberg et al., 2002). Seizure spreading has

been shown to result in glutamatergic excitotoxicity within the regions involved in the epileptic network, eventually resulting in neuronal death and dysfunction of inhibitory GABA-A-ergic interneurons (Bernhardt et al., 2009; Sanabria et al., 2002; Zilles et al., 1999). Ultimately, dysfunctional GABA-A-ergic activity may contribute to the maintenance of epileptic activity within areas of seizure spreading (Ragozzino et al., 2005), likely potentiating distant excitotoxicity and concomitant neuronal death. Another possible explanation for the distant cortical atrophy may come from the loss of input from the region of the epileptic focus, resulting in deafferentation and neuronal loss (Bonilha et al., 2010a). Even though these hypotheses originate from studies in TLE, the rationale stems from a dysfunctional epileptic network involving white matter tracts connecting various cortical areas and can therefore also be applied to extra-temporal epilepsies. It is reasonable to believe that the observed atrophy in patients with OIE may result from the same pathological processes affecting a widespread cortical network structurally connected to the insula and its operculae.

Comparing patients with OIE and HCs revealed a widespread pattern of cortical thinning involving all four lobes. Whether these changes have a clinical correlate is unclear but, interestingly, recent studies have identified various neuropsychological deficits in patients with long-standing OIE or patients assessed several months/years after limited damage (in appearance at least) to the operculo-insular area from an ischemic stroke or surgical resection(Baier et al., 2013; Bamiou et al., 2006; Clark et al., 2014; Dronkers, 1996; Mak et al., 2005; Von Siebenthal et al., 2016). For instance, insular damage resulting from focal brain lesions or surgical resection has been associated with various cognitive biases affecting decision-making and impairments in sensitivity to expected value when choosing between risky or safe decisions (Clark et al., 2014; Von Siebenthal et al., 2016). In our study, CT of subregions of the orbito-frontal area, a key region in reward/decision-making circuitry that is functionally and structurally connected to the anterior insula (Canessa et al., 2013; Deen et al., 2011; Ghaziri et al., 2017), was remarkably decreased in patients with OIE. Deficits in temperature perception have also been reported following unilateral damage to the posterior insula (Baier et al., 2014). It is conceivable that the significant perirolandic atrophy found in our study might partially contribute to this deficit in sensorimotor processing. Our group also previously reported the neuropsychological performance in 18 patients with OIE before and after partial or complete insulectomy (Boucher et al., 2015a). In this study, preoperative neuropsychological assessment revealed that verbal fluency, picture naming and verbal memory encoding were consistently altered in patients with left OIE whereas visuospatial memory encoding was impaired in patients with right OIEs (Boucher et al., 2015a). Interestingly, our study revealed notable cortical atrophy in mesiotemporal and lateral temporal regions mainly ipsilateral but also contralateral to the seizure focus. Finally, impairment in recognition of facial expressions was observed in patients with insular penetrating brain injuries (Boucher et al., 2015b; Dal Monte et al., 2013). Mild occipital atrophy was detected in patients with OIE, potentially contributing to the deficits in visual processing. Whether these neuropsychological deficits are in part explained by subtle damage to areas connected to the insula is purely speculative at this time. Nevertheless, the multimodal functions of the insula and its extensive multilobar structural connections combined with the consistent recruitment of diffuse cortical regions during insular-activating tasks in fMRI studies suggest that extra-insular dysfunction could possibly contribute to the neuropsychological deficits observed in patients with insular damage from various causes including OIE.

The pattern of cortical atrophy in OIE as compared with TLE seems to correspond with the more widespread connections of the insula to adjacent lobes. Patients with TLE were included on the basis of the presence of hippocampal sclerosis and concordant semiology and non-invasive investigations. We would therefore expect to observe more significant atrophy of the mesiotemporal structures in patients with TLE. However, we unexpectedly noted more cortical thinning within this region in patients with OIE than TLE. A possible explanation for this conflicting finding may be related to the difficulty in precisely identifying pure operculo-insular foci. Patients with suspected insular epileptic foci may in fact exhibit a larger epileptogenic zone that may also involve the mesiotemporal structures (i.e. temporo-insular epilepsy) (Barba et al., 2007, 2017). In our study, invasive monitoring was performed in most patients (13/14) and seizure control was observed in all OIE participants (Engel I/II), suggesting that the epileptic focus may rightfully originate from the insula or its operculae. Furthermore, the duration of epilepsy was similar in both groups and therefore the severity of epilepsy in OIE patients is an improbable explanation for these findings. Alternatively, we believe that the limited resolution of MRI may have resulted in overlapping voxels between the insular cortex and the mesiotemporal structures, two areas only separated by a few millimeters, therefore falsely attributing subregions to the wrong area on the template during normalization.

The present study provides unique information regarding the pattern of cortical atrophy observed in patients with OIE. It is however limited by the number of subjects, which is at least in part attributed to the rarity of OIE. To overcome this limitation, patients with both lesional and non-lesional OIE were combined in the analysis. In this regard, the three patients with insular cortical dysplasia could potentially have increased the CT focally and influence the between-group analysis. However, we observed atrophy within the insula, and excluding those patients who typically exhibit local increase in CT in areas of cortical dysplasia would likely have reinforced our findings. In addition, the anterior and posterior insulae seem to present a differential pattern of connectivity. Various functional and structural connectivity studies have shown that the anterior insula is highly linked to the anterior cingulate gyrus, the orbitofrontal cortex and the prefrontal area whereas the posterior insula is more connected to the perirolandic, parietal and temporoparietal cortices (Almashaikhi et al., 2014; Cauda et al., 2012; Cerliani et al., 2012; Deen et al., 2011; Ghaziri et al., 2017; Zerouali et al., 2016).In our study, the epileptogenic focus involved either the anterior, posterior, or the whole extent of the insula. It is therefore conceivable that foci within different subregions of the insula might have resulted in distinctive connectivity-related distributions of atrophy.

Despite these drawbacks, the rarity of pure OIEs drove the inclusion and clustering of all patients into a unique group with the aim of optimizing the statistical comparison. Furthermore, patients with right-sided OIE or TLE were side-flipped, allowing the analysis to be performed uniformly. Side-flipping in patients with a unilateral epileptic focus is a frequently performed step in quantitative MRI studies (Keller et al., 2015; Yasuda et al., 2010). Such data pooling enables to improve statistical power and facilitates detection of atrophic regions (Yasuda et al., 2010). A potential limitation lies in the asymmetrical brain atrophy sometimes observed in TLE, revealing a more widespread atrophy in dominant hemisphere TLE (Kemmotsu et al., 2011; Liu et al., 2016). While this issue is justified in TLE subjects, the inter-hemispheric difference is less marked in OIE subjects for which both structural and functional MRI studies revealed a more similar, albeit not identical, insular connectivity pattern (Cerliani et al., 2012; Deen et al., 2011; Ghaziri et al., 2017). It is therefore conceivable that cortico-cortical insular connections would lead to homologous distribution of cortical atrophy regardless of the side of seizure onset.

Like any neuroimaging tools, ANTs uses the best information it can acquire from the data it is analyzing. Hence, the main limitations are the resolution of the maps, restraining the ability to appropriately map the sulco-gyral anatomy of the regions, as well as the accurate classification of cortical tissues such as white and gray matter in areas heavily myelinated. Other limitations include the smoothness of the images, which reduces the spatial resolution, the different image acquisition protocols and the diverse data processing (Han et al., 2006). In addition, subjective differences such as subjective plasticity or heredity may also play a role (He et al., 2007).

Furthermore, we used a linear model to assess differences between groups, while the brain appears to be changing in a non-linear way, and differently between regions (Sowell et al., 2003). However, with the current number of participants, it would be difficult to run a non-linear analysis, and it is recommended to first assess linear changes and explore non-linear components later with more participants. Another limitation is performing the analysis in the volume and then projecting it to a 3D representation of the surface of the brain. Indeed, because of smoothing and coregistration approximations, part of a significant region may be projected on the wrong gyri and create a spurious cluster (Das et al., 2009). However, we reported the significant regions automatically with xjview on volumic data and 3D representations serve only a visualisation purpose.

5. Conclusion

Our results reveal, for the first time, insular and diffuse extra-insular atrophy in patients with OIE. The pattern of atrophy in OIE included the insula and adjacent operculae, the orbitofrontal, mesiotemporal and lateral temporal cortices as well as the perirolandic region. In addition, contrasting the CT in patients with OIE and TLE revealed a more significant atrophy in the former. Obviously, these preliminary observations will need to be reproduced in larger studies. Future studies should also attempt to establish if these morphological changes are related to epileptic activity and propagation patterns.

Acknowledgements

The authors would like to thank the staff of the Neuroimaging Unit at the Centre Hospitalier de l'Université de Montréal (CHUM) for their technical assistance. The authors would also like to thank the Savoy Foundation for Epilepsy and the Fonds de Recherche du Québec - Santé (32071) for their financial support through scholarships awarded to the main author.

Funding

This work was supported by the Quebec Bio-Imaging Network (5886), the Canadian Institute of Health Research(CIHR; MOP-BSC-343410-97930-DLGNH) and the Natural Sciences and Engineering Research Council of Canada (RGPIN-2016-05216N).

Disclosure

Authors report no conflict of interest.

References

Almashaikhi, T., Rheims, S., Jung, J., Ostrowsky-Coste, K., Montavont, A., De Bellescize, J., Arzimanoglou, A., Keo Kosal, P., Guénot, M., Bertrand, O., Ryvlin, P., 2014. Functional connectivity of insular efferences. Hum. Brain Mapp. 5294, 5279–5294. http://dx.doi.org/10.1002/hbm.22549.

Alomar, S., Mullin, J.P., Smithason, S., Gonzalez-Martinez, J., 2017. Indications, technique, and safety profile of insular stereoelectroencephalography electrode implantation in medically intractable epilepsy. J. Neurosurg. 35, 1–11. http://dx.doi.org/10.3171/2017.1.JNS161070.

Ashburner, J., Friston, K.J., 2000. Voxel-based morphometry–the methods. NeuroImage 11, 805–821. http://dx.doi.org/10.1006/nimg.2000.0582.

Avants, B.B., Epstein, C.L., Grossman, M., Gee, J.C., 2008. Symmetric diffeomorphic image registration with cross-correlation: evaluating automated labeling of elderly and neurodegenerative brain. Med. Image Anal. 12, 26–41. http://dx.doi.org/10.1016/j.media.2007.06.004.

Avants, B.B., Tustison, N.J., Song, G., Cook, P.a., Klein, A., Gee, J.C., 2011. A reproducible evaluation of ANTs similarity metric performance in brain image registration. NeuroImage 54, 2033–2044. http://dx.doi.org/10.1016/j.neuroimage.2010.09.025.

Baier, B., Conrad, J., Zu Eulenburg, P., Best, C., Müller-Forell, W., Birklein, F., Dieterich, M., 2013. Insular strokes cause no vestibular deficits. Stroke 44, 2604–2606. http://dx.doi.org/10.1161/STROKEAHA.113.001816.

Baier, B., zu Eulenburg, P., Geber, C., Rohde, F., Rolke, R., Maihöfner, C., Birklein, F., Dieterich, M., 2014. Insula and sensory insular cortex and somatosensory control in patients with insular stroke. Eur. J. Pain 18, 1385–1393. http://dx.doi.org/10.1002/j.1532-2149.2014.501.x.

Bamiou, D.-E., Musiek, F.E., Stow, I., Stevens, J., Cipolotti, L., Brown, M.M., Luxon, L.M., 2006. Auditory temporal processing deficits in patients with insular stroke. Neurology 67, 614–619. http://dx.doi.org/10.1212/01.wnl.0000230197.40410.db.

Barba, C., Barbati, G., Minotti, L., Hoffmann, D., Kahane, P., 2007. Ictal clinical and scalp-EEG findings differentiating temporal lobe epilepsies from temporal “plus” epilepsies. Brain 130, 1957–1967. http://dx.doi.org/10.1093/brain/awm108.

Barba, C., Minotti, L., Job, A.-S., Kahane, P., 2017. The insula in temporal plus epilepsy. J. Clin. Neurophysiol. 34, 324–327. http://dx.doi.org/10.1097/WNP.0000000000000389.

Bernhardt, B.C., Worsley, K.J., Besson, P., Concha, L., Lerch, J.P., Evans, A.C., Bernasconi, N., 2008. Mapping limbic network organization in temporal lobe epilepsy using morphometric correlations: insights on the relation between mesiotemporal connectivity and cortical atrophy. NeuroImage 42, 515–524. http://dx.doi.org/10.1016/j.neuroimage.2008.04.261.

Bernhardt, B.C., Worsley, K.J., Kim, H., Evans, A.C., Bernasconi, A., Bernasconi, N., 2009. Longitudinal and cross-sectional analysis of atrophy in pharmacoresistant temporal lobe epilepsy. Neurology 72, 1747–1754. http://dx.doi.org/10.1212/01.wnl.0000345969.57574.f5.

Bernhardt, B.C., Bernasconi, N., Concha, L., Bernasconi, A., 2010. Cortical thickness analysis in temporal lobe epilepsy: reproducibility and relation to outcome. Neurology 74, 1776–1784. http://dx.doi.org/10.1212/WNL.0b013e3181e0f80a.

Bonilha, L., Edwards, J.C., Kinsman, S.L., Morgan, P.S., Fridriksson, J., Rorden, C., Rumboldt, Z., Roberts, D.R., Eckert, M.A., Halford, J.J., 2010a. Extrahippocampal gray matter loss and hippocampal deafferentation in patients with temporal lobe epilepsy. Epilepsia 51, 519–528. http://dx.doi.org/10.1111/j.1528-1167.2009.02506.x.

Bonilha, L., Elm, J.J., Edwards, J.C., Morgan, P.S., Hicks, C., Lozar, C., Rumboldt, Z., Roberts, D.R., Rorden, C., Eckert, M.A., 2010b. How common is brain atrophy in patients with medial temporal lobe epilepsy? Epilepsia 51, 1774–1779. http://dx.doi.org/10.1111/j.1528-1167.2010.02576.x.

Bookstein, F.L., 2001. “Voxel-based morphometry” should not be used with imperfectly registered images. NeuroImage 14, 1454–1462. http://dx.doi.org/10.1006/NIMG.2001.0770.

Boucher, O., Rouleau, I., Escudier, F., Malenfant, A., Denault, C., Charbonneau, S., Finet, P., Lassonde, M., Lepore, F., Bouthillier, A., Nguyen, D.K., 2015a. Neuropsychological performance before and after partial or complete insulectomy in patients with epilepsy. Epilepsy Behav. 43, 53–60. http://dx.doi.org/10.1016/j.yebeh.2014.11.016.

Boucher, O., Rouleau, I., Lassonde, M., Lepore, F., Bouthillier, A., Nguyen, D.K., 2015b. Social information processing following resection of the insular cortex. Neuropsychologia 71, 1–10. http://dx.doi.org/10.1016/j.neuropsychologia.2015.03.008.

Bouthillier, A., Nguyen, D.K., 2017. Epilepsy surgeries requiring an operculoinsular cortectomy: operative technique and results. Neurosurgery 81, 602–612. http://dx.doi.org/10.1093/neuros/nyx080.

Canessa, N., Crespi, C., Motterlini, M., Baud-Bovy, G., Chierchia, G., Pantaleo, G., Tettamanti, M., Cappa, S.F., 2013. The functional and structural neural basis of individual differences in loss aversion. J. Neurosci. 33, 14307–14317. http://dx.doi.org/10.1523/JNEUROSCI.0497-13.2013.

Cauda, F., Agata, F.D., Sacco, K., Duca, S., Geminiani, G., Vercelli, A., D'Agata, F., Sacco, K., Duca, S., Geminiani, G., Vercelli, A., 2011. Functional connectivity of the insula in the resting brain. NeuroImage 55, 8–23. http://dx.doi.org/10.1016/j.neuroimage.2010.11.049.

Cauda, F., Costa, T., Torta, D.M.E., Sacco, K., D'Agata, F., Duca, S., Geminiani, G., Fox, P.T., Vercelli, A., 2012. Meta-analytic clustering of the insular cortex. Characterizing the meta-analytic connectivity of the insula when involved in active tasks. NeuroImage 62, 343–355. http://dx.doi.org/10.1016/j.neuroimage.2012.04.012.

Cauda, F., Geminiani, G.C., Vercelli, A., 2014. Evolutionary appearance of von Economo's neurons in the mammalian cerebral cortex. Front. Hum. Neurosci. 8 (104). http://dx.doi.org/10.3389/fnhum.2014.00104.

Cerliani, L., Thomas, R.M., Jbabdi, S., Siero, J.C.W., Nanetti, L., Crippa, A., Gazzola, V., D'Arceuil, H., Keysers, C., 2012. Probabilistic tractography recovers a rostrocaudal trajectory of connectivity variability in the human insular cortex. Hum. Brain Mapp. 33, 2005–2034. http://dx.doi.org/10.1002/hbm.21338.

Clark, L., Studer, B., Bruss, J., Tranel, D., Bechara, A., 2014. Damage to insula abolishes cognitive distortions during simulated gambling. Proc. Natl. Acad. Sci. U. S. A. 111, 6098–6103. http://dx.doi.org/10.1073/pnas.1322295111.

Cloutman, L.L., Binney, R.J., Drakesmith, M., Parker, G.J.M., Lambon Ralph, M.A., 2012. The variation of function across the human insula mirrors its patterns of structural connectivity: evidence from in vivo probabilistic tractography. NeuroImage 59, 3514–3521. http://dx.doi.org/10.1016/j.neuroimage.2011.11.016.

Coan, A.C., Campos, B.M., Yasuda, C.L., Kubota, B.Y., Bergo, F.P., Guerreiro, C.A., Cendes, F., 2014. Frequent seizures are associated with a network of gray matter atrophy in temporal lobe epilepsy with or without hippocampal sclerosis. PLoS One 9, e85843. http://dx.doi.org/10.1371/journal.pone.0085843.

Dal Monte, O., Krueger, F., Solomon, J.M., Schintu, S., Knutson, K.M., Strenziok, M., Pardini, M., Leopold, A., Raymont, V., Grafman, J., 2013. A voxel-based lesion study on facial emotion recognition after penetrating brain injury. Soc. Cogn. Affect. Neurosci. 8, 632–639. http://dx.doi.org/10.1093/scan/nss041.

Dale, A.M., Fischl, B., Sereno, M.I., 1999. Cortical surface-based analysis. I. Segmentation and surface reconstruction. Neuroimage 9, 179–194. http://dx.doi.org/10.1006/nimg.1998.0395.

Das, S.R., Avants, B.B., Grossman, M., Gee, J.C., 2009. Registration based cortical thickness measurement. NeuroImage 45, 867–879. http://dx.doi.org/10.1016/j.neuroimage.2008.12.016.

Deen, B., Pitskel, N.B., Pelphrey, K.a., 2011. Three systems of insular functional

connectivity identified with cluster analysis. Cereb. Cortex 21, 1498–1506. http://dx.doi.org/10.1093/cercor/bhq186.
Dronkers, N.F., 1996. A new brain region for coordinating speech articulation. Nature 384, 159–161. http://dx.doi.org/10.1038/384159a0.
Freri, E., Matricardi, S., Gozzo, F., Cossu, M., Granata, T., Tassi, L., 2017. Perisylvian, including insular, childhood epilepsy: Presurgical workup and surgical outcome. Epilepsia 58, 1360–1369. http://dx.doi.org/10.1111/epi.13816.
Ghaziri, J., Tucholka, A., Girard, G., Houde, J.-C., Boucher, O., Gilbert, G., Descoteaux, M., Lippé, S., Rainville, P., Nguyen, D.K., 2017. The corticocortical structural connectivity of the human insula. Cereb. Cortex 27, 1216–1228. http://dx.doi.org/10.1093/cercor/bhv308.
Gras-Combe, G., Minotti, L., Hoffmann, D., Krainik, A., Kahane, P., Chabardes, S., 2016. Surgery for nontumoral insular epilepsy explored by Stereoelectroencephalography. Neurosurgery 79, 578–588. http://dx.doi.org/10.1227/NEU.0000000000001257.
Han, X., Jovicich, J., Salat, D., van der Kouwe, A., Quinn, B., Czanner, S., Busa, E., Pacheco, J., Albert, M., Killiany, R., Maguire, P., Rosas, D., Makris, N., Dale, A., Dickerson, B., Fischl, B., 2006. Reliability of MRI-derived measurements of human cerebral cortical thickness: the effects of field strength, scanner upgrade and manufacturer. NeuroImage 32, 180–194. http://dx.doi.org/10.1016/j.neuroimage.2006.02.051.
He, Y., Chen, Z.J., Evans, A.C., 2007. Small-world anatomical networks in the human brain revealed by cortical thickness from MRI. Cereb. Cortex 17, 2407–2419. http://dx.doi.org/10.1093/cercor/bhl149.
Isnard, J., Guénot, M., Ostrowsky, K., Sindou, M., Mauguière, F., 2000. The role of the insular cortex in temporal lobe epilepsy. Ann. Neurol. 48, 614–623.
Jakab, A., Molnár, P.P., Bogner, P., Béres, M., Berényi, E.L., 2012. Connectivity-based parcellation reveals interhemispheric differences in the insula. Brain Topogr. 25, 264–271. http://dx.doi.org/10.1007/s10548-011-0205-y.
Keller, S.S., Richardson, M.P., O'Muircheartaigh, J., Schoene-Bake, J.-C., Elger, C., Weber, B., 2015. Morphometric MRI alterations and postoperative seizure control in refractory temporal lobe epilepsy. Hum. Brain Mapp. 36, 1637–1647. http://dx.doi.org/10.1002/hbm.22722.
Kemmotsu, N., Girard, H.M., Bernhardt, B.C., Bonilha, L., Lin, J.J., Tecoma, E.S., Iragui, V.J., Hagler, D.J., Halgren, E., McDonald, C.R., 2011. MRI analysis in temporal lobe epilepsy: cortical thinning and white matter disruptions are related to side of seizure onset. Epilepsia 52, 2257–2266. http://dx.doi.org/10.1111/j.1528-1167.2011.03278.x.
Klein, A., Andersson, J., Ardekani, B.a., Ashburner, J., Avants, B., Chiang, M.C., Christensen, G.E., Collins, D.L., Gee, J., Hellier, P., Song, J.H., Jenkinson, M., Lepage, C., Rueckert, D., Thompson, P., Vercauteren, T., Woods, R.P., Mann, J.J., Parsey, R.V., 2009. Evaluation of 14 nonlinear deformation algorithms applied to human brain MRI registration. NeuroImage 46, 786–802. http://dx.doi.org/10.1016/j.neuroimage.2008.12.037.
Li, J., Zhang, Z., Shang, H., 2012. A meta-analysis of voxel-based morphometry studies on unilateral refractory temporal lobe epilepsy. Epilepsy Res. 98, 97–103. http://dx.doi.org/10.1016/j.eplepsyres.2011.10.002.
Lin, J.J., Salamon, N., Lee, A.D., Dutton, R.A., Geaga, J.A., Hayashi, K.M., Luders, E., Toga, A.W., Engel, J., Thompson, P.M., 2007. Reduced neocortical thickness and complexity mapped in mesial temporal lobe epilepsy with hippocampal sclerosis. Cereb. Cortex 17, 2007–2018. http://dx.doi.org/10.1093/cercor/bhl109.
Liu, M., Bernhardt, B.C., Bernasconi, A., Bernasconi, N., 2016. Gray matter structural compromise is equally distributed in left and right temporal lobe epilepsy. Hum. Brain Mapp. 37, 515–524. http://dx.doi.org/10.1002/hbm.23046.
Mak, Y.E., Simmons, K.B., Gitelman, D.R., Small, D.M., 2005. Taste and olfactory intensity perception changes following left insular stroke. Behav. Neurosci. 119, 1693–1700. http://dx.doi.org/10.1037/0735-7044.119.6.1693.
Malak, R., Bouthillier, A., Carmant, L., Cossette, P., Giard, N., Saint-Hilaire, J.-M., Nguyen, D.K.D.B.D.K.D.B., Nguyen, D.K.D.B.D.K.D.B., Hospitalier, C., Hospital, N., Object, C., 2009. Microsurgery of epileptic foci in the insular region. J. Neurosurg. 110, 1153–1163. http://dx.doi.org/10.3171/2009.1.JNS08807.
McDonald, C.R., Hagler, D.J., Ahmadi, M.E., Tecoma, E., Iragui, V., Gharapetian, L., Dale, A.M., Halgren, E., 2008. Regional neocortical thinning in mesial temporal lobe epilepsy. Epilepsia 49, 794–803. http://dx.doi.org/10.1111/j.1528-1167.2008.01539.x.
Mechelli, A., Price, C., Friston, K., Ashburner, J., 2005. Voxel-based morphometry of the human brain: methods and applications. Curr. Med. Imaging Rev. 1, 105–113. http://dx.doi.org/10.2174/1573405054038726.
Mesulam, M.M., Mufson, E.J., 1982. Insula of the old world monkey. III: efferent cortical output and comments on function. J. Comp. Neurol. 212, 38–52. http://dx.doi.org/10.1002/cne.902120104.
Mohamed, I.S., Gibbs, S.A., Robert, M., Bouthillier, A., Leroux, J.M., Nguyen, D.K., 2013. The utility of magnetoencephalography in the presurgical evaluation of refractory insular epilepsy. Epilepsia 54, 1950–1959. http://dx.doi.org/10.1111/epi.12376.
Mufson, E.J., Mesulam, M.M., 1982. Insula of the old world monkey. II: afferent cortical input and comments on the claustrum. J. Comp. Neurol. 212, 23–37. http://dx.doi.org/10.1002/cne.902120103.
Nguyen, D.K., Nguyen, D.B., Malak, R., Leroux, J.M., Carmant, L., Saint-Hilaire, J.M., Giard, N., Cossette, P., Bouthillier, A., 2009. Revisiting the role of the insula in refractory partial epilepsy. Epilepsia 50, 510–520. http://dx.doi.org/10.1111/j.1528-1167.2008.01758.x.
Nieuwenhuys, R., 2012. The insular cortex: a review. Prog. Brain Res. 195, 123–163. http://dx.doi.org/10.1016/B978-0-444-53860-4.00007-6.
Obaid, S., Zerouali, Y., Nguyen, D.K., 2017. Insular epilepsy: semiology and noninvasive investigations. J. Clin. Neurophysiol. 34, 315–323. http://dx.doi.org/10.1111/epi.13682.
Ostrowsky, K., Isnard, J., Ryvlin, P., Guénot, M., Fischer, C., Mauguière, F., 2000. Functional mapping of the insular cortex: clinical implication in temporal lobe epilepsy. Epilepsia 41, 681–686. http://dx.doi.org/10.1111/j.1528-1157.2000.tb00228.x.
Ragozzino, D., Palma, E., Di Angelantonio, S., Amici, M., Mascia, A., Arcella, A., Giangaspero, F., Cantore, G., Di Gennaro, G., Manfredi, M., Esposito, V., Quarato, P.P., Miledi, R., Eusebi, F., 2005. Rundown of GABA type A receptors is a dysfunction associated with human drug-resistant mesial temporal lobe epilepsy. Proc. Natl. Acad. Sci. U. S. A. 102, 15219–15223. http://dx.doi.org/10.1073/pnas.0507339102.
Ryvlin, P., Minotti, L., Demarquay, G., Hirsch, E., Arzimanoglou, A., Hoffman, D., Guénot, M., Picard, F., Rheims, S., Kahane, P., 2006. Nocturnal hypermotor seizures, suggesting frontal lobe epilepsy, can originate in the insula. Epilepsia 47, 755–765. http://dx.doi.org/10.1111/j.1528-1167.2006.00510.x.
Sanabria, E.R.G., da Silva, A.V., Spreafico, R., Cavalheiro, E.A., 2002. Damage, reorganization, and abnormal neocortical hyperexcitability in the pilocarpine model of temporal lobe epilepsy. Epilepsia 43 (Suppl. 5), 96–106.
Sowell, E.R., Peterson, B.S., Thompson, P.M., Welcome, S.E., Henkenius, A.L., Toga, A.W., 2003. Mapping cortical change across the human life span. Nat. Neurosci. 6, 309–315. http://dx.doi.org/10.1038/nn1008.
Surbeck, W., Bouthillier, A., Nguyen, D.K., 2010. Refractory insular cortex epilepsy: clinical features, investigation and treatment. Future Neurol. 5, 491–499. http://dx.doi.org/10.2217/fnl.10.36.
Thompson, P.M., Hayashi, K.M., Simon, S.L., Geaga, J.A., Hong, M.S., Sui, Y., Lee, J.Y., Toga, A.W., Ling, W., London, E.D., 2004. Structural abnormalities in the brains of human subjects who use methamphetamine. J. Neurosci. 24, 6028–6036. http://dx.doi.org/10.1523/JNEUROSCI.0713-04.2004.
Tustison, N.J., Cook, P.A., Klein, A., Song, G., Das, S.R., Duda, J.T., Kandel, B.M., van Strien, N., Stone, J.R., Gee, J.C., Avants, B.B., 2014. Large-scale evaluation of ANTs and FreeSurfer cortical thickness measurements. NeuroImage 99, 166–179. http://dx.doi.org/10.1016/J.NEUROIMAGE.2014.05.044.
Uddin, L.Q.L.Q.L.Q., Nomi, J.S., Hébert-Seropian, B., Ghaziri, J., Boucher, O., 2017. Structure and function of the human insula. J. Clin. Neurophysiol. 34, 300–306. http://dx.doi.org/10.1097/WNP.0000000000000377.
Von Siebenthal, Z., Boucher, O., Rouleau, I., Lassonde, M., Lepore, F., Nguyen, D.K., 2016. Decision-making impairments following insular and medial temporal lobe resection for drug-resistant epilepsy. Soc. Cogn. Affect. Neurosci. 12, nsw152. http://dx.doi.org/10.1093/scan/nsw152.
Weil, A.G., Fallah, A., Lewis, E.C., Bhatia, S., 2016. Medically resistant pediatric insular-opercular/perisylvian epilepsy. Part 1: invasive monitoring using the parasagittal transinsular apex depth electrode. J. Neurosurg. Pediatr. 18, 511–522. http://dx.doi.org/10.3171/2016.4.PEDS15636.
Wennberg, R., Arruda, F., Quesney, L.F., Olivier, A., 2002. Preeminence of extrahippocampal structures in the generation of mesial temporal seizures: evidence from human depth electrode recordings. Epilepsia 43, 716–726.
Whelan, C.D., Altmann, A., Botía, J.A., Jahanshad, N., Hibar, D.P., Absil, J., Alhusaini, S., Alvim, M.K.M., Auvinen, P., Bartolini, E., Bergo, F.P.G., Bernardes, T., Blackmon, K., Braga, B., Caligiuri, M.E., Calvo, A., Carr, S.J., Chen, J., Chen, S., Cherubini, A., David, P., Domin, M., Foley, S., França, W., Haaker, G., Isaev, D., Keller, S.S., Kotikalapudi, R., Kowalczyk, M.A., Kuzniecky, R., Langner, S., Lenge, M., Leyden, K.M., Liu, M., Loi, R.Q., Martin, P., Mascalchi, M., Morita, M.E., Pariente, J.C., Rodríguez-Cruces, R., Rummel, C., Saavalainen, T., Semmelroch, M.K., Severino, M., Thomas, R.H., Tondelli, M., Tortora, D., Vaudano, A.E., Vivash, L., von Podewils, F., Wagner, J., Weber, B., Yao, Y., Yasuda, C.L., Zhang, G., Bargalló, N., Bender, B., Bernasconi, N., Bernasconi, A., Bernhardt, B.C., Blümcke, I., Carlson, C., Cavalleri, G.L., Cendes, F., Concha, L., Delanty, N., Depondt, C., Devinsky, O., Doherty, C.P., Focke, N.K., Gambardella, A., Guerrini, R., Hamandi, K., Jackson, G.D., Kälviäinen, R., Kochunov, P., Kwan, P., Labate, A., McDonald, C.R., Meletti, S., O'Brien, T.J., Ourselin, S., Richardson, M.P., Striano, P., Thesen, T., Wiest, R., Zhang, J., Vezzani, A., Ryten, M., Thompson, P.M., Sisodiya, S.M., 2018. Structural brain abnormalities in the common epilepsies assessed in a worldwide ENIGMA study. Brain 141, 391–408. http://dx.doi.org/10.1093/brain/awx341.
Yasuda, C.L., Betting, L.E., Cendes, F., 2010. Voxel-based morphometry and epilepsy. Expert. Rev. Neurother. 10, 975–984. http://dx.doi.org/10.1586/ern.10.63.
Zerouali, Y., Pouliot, P., Robert, M., Mohamed, I., Bouthillier, A., Lesage, F., Nguyen, D.K., 2016. Magnetoencephalographic signatures of insular epileptic spikes based on functional connectivity. Hum. Brain Mapp. 0. http://dx.doi.org/10.1002/hbm.23238.
Zilles, K., Qü, M.S., Köhling, R., Speckmann, E.J., 1999. Ionotropic glutamate and GABA receptors in human epileptic neocortical tissue: quantitative in vitro receptor autoradiography. Neuroscience 94, 1051–1061.